

# The Thioredoxin System Reduces Protein Persulfide Intermediates Formed during the Synthesis of Thio-Cofactors in *Bacillus subtilis*

Chenkang Zheng,<sup>†</sup> Selina Guo,<sup>†</sup> William G. Tennant,<sup>†</sup> Pradyumna K. Pradhan,<sup>†,‡</sup> Katherine A. Black,<sup>\*,†,§</sup> and Patricia C. Dos Santos<sup>\*,†</sup>

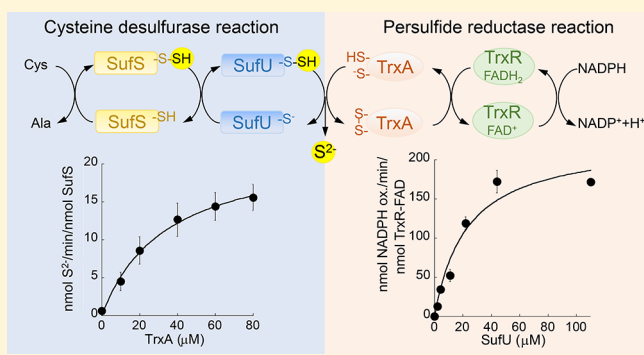
<sup>†</sup>Department of Chemistry, Wake Forest University, Winston-Salem, North Carolina 27106, United States

<sup>‡</sup>Department of Chemistry and Biochemistry, The University of North Carolina at Greensboro, Greensboro, North Carolina 27412, United States

<sup>§</sup>Department of Medicine, Weill Cornell Medicine, New York, New York 10065, United States

## Supporting Information

**ABSTRACT:** The biosynthesis of Fe–S clusters and other thio-cofactors requires the participation of redox agents. A shared feature in these pathways is the formation of transient protein persulfides, which are susceptible to reduction by artificial reducing agents commonly used in reactions *in vitro*. These agents modulate the reactivity and catalytic efficiency of biosynthetic reactions and, in some cases, skew the enzymes' kinetic behavior, bypassing sulfur acceptors known to be critical for the functionality of these pathways *in vivo*. Here, we provide kinetic evidence for the selective reactivity of the *Bacillus subtilis* Trx (thioredoxin) system toward protein-bound persulfide intermediates. Our results demonstrate that the redox flux of the Trx system modulates the rate of sulfide production in cysteine desulfurase assays. Likewise, the activity of the Trx system is dependent on the rate of persulfide formation, suggesting the occurrence of coupled reaction schemes between both enzymatic systems *in vitro*. Inactivation of TrxA (thioredoxin) or TrxR (thioredoxin reductase) impairs the activity of Fe–S enzymes in *B. subtilis*, indicating the involvement of the Trx system in Fe–S cluster metabolism. Surprisingly, biochemical characterization of TrxA reveals that this enzyme is able to coordinate Fe–S species, resulting in the loss of its reductase activity. The inactivation of TrxA through the coordination of a labile cluster, combined with its proposed role as a physiological reducing agent in sulfur transfer pathways, suggests a model for redox regulation. These findings provide a potential link between redox regulation and Fe–S metabolism.



The biosynthesis of Fe–S clusters and other thio-cofactors requires specialized pathways and redox agents. In eukaryotes and bacteria, the free amino acid cysteine serves as the sulfur source for the synthesis of nearly all known thio-cofactors.<sup>1,2</sup> In these pathways, cysteine desulfurases are responsible for the initial activation and mobilization of sulfur. Enzymes of this class use the pyridoxal 5'-phosphate (PLP) cofactor to catalyze the cleavage of the C–S bond from cysteine and subsequently transfer sulfur to downstream sulfur acceptor proteins. The reaction mechanism involves two major steps. The mandatory formation of a persulfide intermediate on the enzyme's active site cysteine residue marks the halfway point of the sulfur transfer reaction.<sup>2,3</sup> The reaction is then completed upon the release of the first product, alanine, followed by the second committed step, the transfer of the persulfide sulfur to an acceptor protein.<sup>4</sup> Detailed kinetic, labeling, and inhibition studies have characterized the chemical events in the first half of the reaction leading to the formation of the cysteine desulfurase enzyme–persulfide intermediate.<sup>3,5–7</sup> The sequence of reaction steps leading to this enzyme intermediate is proposed to be identical among all members of

this enzyme group, whereas the transfer of the persulfide is controlled by their sulfur acceptor molecules.<sup>4</sup> The interactions between cysteine desulfurases and sulfur acceptors are proposed to restrict the reactivity of these enzymes and direct the flow of sulfur transfer to selected thio-cofactor pathways.<sup>8–14</sup>

The transfer of sulfur from cysteine desulfurases to sulfur acceptor proteins is possible in the absence of a reductant; however, the following sulfur transfer events or subsequent steps for incorporation into thio-cofactors require a reducing agent under turnover conditions. Specifically, for Fe–S cluster biogenesis, a physiological reductant is necessary to reduce the persulfide sulfur (S<sup>0</sup>) to sulfide (S<sup>2-</sup>), the formal charge of sulfur in Fe–S clusters. Consequently, previous *in vitro* kinetic analyses conducted in the presence and absence of sulfur acceptors have mainly been performed in reaction mixtures

Received: January 17, 2019

Revised: February 27, 2019

Published: March 11, 2019

containing artificial reducing agents (e.g., dithiothreitol, a typical component of assay mixtures).<sup>6,11,15–17</sup> The problem with the use of these artificial reducing agents is that they affect the kinetic profile of cysteine desulfurase and sulfur acceptor reactions. Under these conditions, the persulfide enzyme intermediate residing on the cysteine desulfurase and/or sulfur acceptor can be directly reduced, consequently releasing sulfide and resetting these enzymatic components for the next catalytic cycle. The concentration and type of reducing agent (e.g., DTT, TCEP, GSH, and ferredoxin) used in assay reactions not only lead to differences in activities but also can alter the overall reaction scheme.<sup>5,18,19</sup> In particular, the reduction of persulfide intermediates directly impacts the enzyme's turnover rate and, in some cases, precludes sulfur transfer from the enzyme to sulfur acceptors.<sup>12</sup> Such distinct reactivities challenge the proposed kinetic schemes for these enzymes, making it difficult to reconstruct biologically relevant sulfur mobilization pathways *in vitro*. While the use of artificial agents has enabled initial characterization of these enzymes, this experimental methodology does not inform about the susceptibility of persulfide intermediates to reaction with physiological reducing agents.

In previous work, we have investigated sulfur transfer reactions between cysteine desulfurases and sulfur acceptors from the model Gram-positive bacterium *Bacillus subtilis*.<sup>20,21</sup> These enzymes display targeted specificities toward their sulfur acceptor proteins, and intra- or interspecies cross reactivity has not yet been reported.<sup>12,13,22</sup> In this model, sulfur transfer reactions are proposed to be the result of specific protein–protein interactions.<sup>23</sup> Genetic analysis suggests that *in vivo* physiological reducing agents are not able to bypass the requirement of sulfur acceptors.<sup>22,24</sup> In Gram-negative and eukaryotic species, physiological reductants GSH and ferredoxin participate in pathways involving cysteine desulfurases.<sup>25,26</sup> *In vivo* studies have demonstrated that elimination of either of these redox agents impairs the biosynthesis of Fe–S clusters, attributing their redox roles to one or more steps in the biosynthetic process.<sup>27–29</sup> Kinetic analysis showed that GSH is competent in reducing persulfides or polysulfides formed on SufE, the specific sulfur acceptor of the *Escherichia coli* cysteine desulfurase, SufS.<sup>18</sup> Ferredoxin is able to interact with cysteine desulfurases, leading to enhancement of the rate of sulfide production and Fe–S cluster formation.<sup>30,31</sup> However, *B. subtilis* does not produce or use GSH and its genome lacks the *isc*-like ferredoxin gene that is associated with thio-cofactor synthesis in species utilizing the *Isc* system.

*B. subtilis*, along with a number of firmicute species, produces bacillithiol (BSH), a low-molecular weight thiol involved in protection against metal, superoxide, salt, and acid stresses.<sup>32</sup> Although BSH is not an essential biothiol, deletion of its biosynthetic genes affects the levels of Fe–S enzymes, depletes the levels of NADPH, and impairs sporulation.<sup>33–36</sup> The dispensable role of BSH suggests that other physiological reducing agents play dominant redox roles. In addition to low-molecular weight thiols, cellular systems utilize oxidoreductases to maintain thiol redox homeostasis.<sup>37,38</sup> Among those, glutaredoxin (Grx) and thioredoxin (Trx) are important agents in promoting the reduction of protein and low-molecular weight mixed disulfides. It is anticipated, however, that Grx-like enzymes are not involved in thiol oxidoreduction reactions in *B. subtilis*. This organism does not utilize GSH,<sup>32</sup> which is intrinsically required in the catalytic cycle of Grx enzymes. In fact, the *B. subtilis* genome encodes only one copy

of a distantly related *grx*-like gene (*ytnI* or *cmoI*) involved in the metabolism of S-methyl cysteine.<sup>39,40</sup>

*B. subtilis* contains one copy of the Trx system, composed of thioredoxin A (TrxA) and its reductase, encoded by *trxA* and *trxB* genes, respectively. Both genes are fully essential for cell viability,<sup>41,42</sup> demonstrating the indispensable role(s) of this oxidoreductase system in *B. subtilis*. Thioredoxin reductase (TrxR) is a member of the pyridine nucleotide-disulfide oxidoreductase family, containing a NADPH binding domain and a redox active disulfide, in addition to its FAD cofactor.<sup>43,44</sup> TrxA is involved in direct reduction of substrates through a reaction cycle involving the formation of a disulfide bond intermediate between the enzyme and substrate.<sup>45</sup> While TrxA is the only protein containing the highly conserved thioredoxin active site WCGPC motif, the *B. subtilis* genome also encodes other non-essential proteins with Trx-like sequences (Figure S1). Among these proteins are the extracytoplasmic disulfide oxidoreductases involved in spore (StoA), biofilm formation (BdbA),<sup>46–48</sup> and NrdH (YosR), a catalytically competent reductant of ribonucleotide reductase.<sup>49</sup> Despite the presence of additional orthologous sequences, both Trx components are considered vital to at least one essential redox reaction in *B. subtilis*.

Proteomic and transcriptomic analyses showed that *trxA* expression is induced by multiple stress conditions and its abundance affects the expression of several genes. The *trxA* gene is induced by heat and salt stress, as well as treatment with ethanol, hydrogen peroxide, or puromycin, conditions necessitating its role in maintaining the native and reduced state of cellular proteins.<sup>42</sup> Downregulation of *trxA* in an IPTG-inducible conditional knockout leads to upregulation of genes involved in sulfur utilization, antioxidant response, sporulation, competence, phage-related functions, endospore formation, and cytochrome *c* synthesis.<sup>50,51</sup> Interestingly, in *B. subtilis*, altered expression of *trxA* impacts the expression of two essential cysteine desulfurases, YrvO and SufS, suggesting a potential link between thioredoxin and life-sustaining sulfur transfer reactions in this organism.<sup>52</sup>

In this study, we assessed the reactivity of the Trx system toward a variety of substrates, including protein persulfides. Kinetic characterization of TrxA showed activity comparable to those of studied systems, in which the two cysteine residues (C29 and C32) are required for the catalytically active form of the reductase. Additionally, we demonstrated that *B. subtilis* TrxA is able to coordinate Fe–S species by means of its catalytic cysteine residues and that the presence of these clusters impacts the reductase activity of the enzyme. The work herein establishes that the Trx system is an effective reductant of persulfides formed as products of reactions involving cysteine desulfurases and sulfur acceptors, such as in the biogenesis of Fe–S clusters and thio-cofactors. Inactivation of this system *in vivo* led to impairment of the activity of enzymes containing Fe–S clusters, suggesting the involvement of the Trx system in Fe–S metabolism. In addition, kinetic analysis showed that the turnover rate of the Trx system is coupled to the rate of sulfur mobilization. That is, the redox flux of the Trx system is mutually coupled to the rate of sulfide production in cysteine desulfurase reactions.

## ■ MATERIALS AND METHODS

**Plasmid Construction.** Coding sequences of *trxA* and *trxB* were amplified through polymerase chain reaction (PCR) using *B. subtilis* wild type (PS832) genomic DNA as the

template. Primers were engineered to contain restriction sites at the 5' and 3' ends of each coding sequence for cloning purposes. Each PCR product was first ligated into the TOPO TA vector (Invitrogen). The PCR products were excised from the TOPO TA vector using restriction digestion and subsequently ligated into the expression vectors listed in Table S1. The correct sequence of all plasmids used in this study was confirmed by DNA sequencing at Genewiz.

**B. subtilis Growth and Enzymatic Assays.** *B. subtilis* PS832 or BEC28500 strains were cultured in LB or Spizizen medium supplemented (MM) with L-tryptophan (10  $\mu\text{g}/\text{mL}$ ), casamino acids (0.05%), L-glutamine (120  $\mu\text{g}/\text{mL}$ ), L-glutamate (120  $\mu\text{g}/\text{mL}$ ), L-leucine (46  $\mu\text{g}/\text{mL}$ ), and L-isoleucine (34  $\mu\text{g}/\text{mL}$ ) at 37 °C while being shaken until a desired OD<sub>600</sub> was reached. For TrxB inhibition, *B. subtilis* PS832 was cultured in the presence of 0.14  $\mu\text{g}/\text{mL}$  (0.5  $\mu\text{M}$ ) ebselen dissolved in dimethyl sulfoxide (DMSO) and compared to cultures treated with DMSO alone as a control. The *B. subtilis* BEC28500 CRISPRi strain was purchased from the Bacillus Genetic Stock Center. This strain contains a copy of the deactivated form of Cas9 under control of the xylose promoter and expresses a sgRNA that hybridizes to *trxA* (on the template strand at positions corresponding to nucleotides 81–101; codons 28–34 on the nontemplate strand) (Table S1). Inactivation of *trxA* transcription was achieved through induction of a deactivated Cas9 upon addition of 1% xylose, as reported previously.<sup>53</sup> Cells were harvested by centrifugation at 12800g for 10 min and frozen at –80 °C until further use.

All assays were performed in an anaerobic glovebox (Coy) equilibrated with 1.5% H<sub>2</sub> and balanced with N<sub>2</sub> gas, according to the protocol of Fang et al., with the following modifications.<sup>33</sup> Cell pellets were washed with 10 mL of degassed buffer A [25 mM Tris-HCl (pH 8), 0.15 M NaCl, and 10% glycerol] followed by centrifugation. The resulting pellets were then resuspended in 10 mL of buffer A and disrupted by an Emulsiflex C5 high-pressure homogenizer (Avestin) at 10000–15000 psi. Cell lysates were collected by centrifugation at 12800g for 20 min and kept in sealed vials on ice for assays. The protein concentration in cell extracts was determined by the Bradford protein assay using BSA as a standard.<sup>54</sup> Glutamate synthase (GOGAT) activity was assayed in 875  $\mu\text{L}$  of a freshly prepared stock mix containing 0.2 M Tris (pH 8), 0.1 M  $\alpha$ -ketoglutarate, 8 mM NADPH, and 75  $\mu\text{L}$  of cell lysate.<sup>55</sup> The initial change in absorbance at 340 nm over time was recorded as S<sub>1</sub>, and the second slope, upon addition of 50  $\mu\text{L}$  of 0.2 M L-glutamine, was recorded as S<sub>2</sub>. The difference in slopes was used to calculate the rate of NADPH consumption using the molar absorption coefficient of 6.22  $\text{mM}^{-1} \text{cm}^{-1}$  as described previously.<sup>33</sup> Isopropylmalate isomerase (LeuCD) assays (1 mL) were initiated by the addition of 1 mM 3-isopropylmalic acid in a reaction mixture buffered with 0.2 M potassium phosphate (pH 7) containing 30  $\mu\text{L}$  of cell lysate. The formation of the intermediate dimethylcitrate was monitored over time through the increase in absorbance at 235 nm, and enzyme activity was calculated using the molar absorption coefficient of 4.668  $\text{mM}^{-1} \text{cm}^{-1}$ .<sup>56,57</sup> Aconitase activity was assessed by monitoring the production of *cis*-aconitate at an absorbance of 240 nm using the molar absorption coefficient of 3.4  $\text{mM}^{-1} \text{cm}^{-1}$ .<sup>58</sup> In detail, 23.5 mM Tris-Na-citrate was mixed with 30  $\mu\text{L}$  of cell lysate in a total reaction volume of 850  $\mu\text{L}$  buffered with 0.1 M Tris (pH 8). The activity of malate dehydrogenase (MDH) was measured by following the consumption of NADH at 340

nm in a 1 mL reaction mixture buffered with 50 mM Tris (pH 7.4) and containing 50  $\mu\text{L}$  of cell lysate, 0.15 mM NADH, and 0.38 mM oxaloacetate. In the threonine dehydrogenase (TDH) assay, cell lysates were spiked with 5 mM L-threonine prior to assay measurements. Each reaction was carried out in the presence of 30  $\mu\text{L}$  of cell lysate, 1.25 mM NAD, and 34 mM L-threonine with 50 mM bicine (pH 8.5) up to a 0.8 mL volume.<sup>59</sup> The activity of TDH was measured and calculated on the basis of the production of NADH at 340 nm. Quercetin 2,3-dioxygenase (QD) activity was quantified by monitoring the decomposition of quercetin over time, using the molar absorption coefficient of 20  $\text{mM}^{-1} \text{cm}^{-1}$  at 367 nm.<sup>60</sup> The enzyme within the cell lysate was stabilized by 4.8  $\mu\text{M}$  quercetin in dimethyl sulfoxide prior to the reaction. Assays (1 mL) were performed by mixing 50  $\mu\text{L}$  of crude extract with 60  $\mu\text{M}$  quercetin in 0.2 M Tris (pH 8) over the course of 2 min.

**Protein Expression and Purification.** Wild type TrxR and TrxA and its variants were expressed from *E. coli* BL21 (DE3) cells transformed with plasmids described in Table S1. TrxR expression was achieved from six 2 L Erlenmeyer flasks, containing 500 mL of LB broth each, whereas TrxA was expressed from 2 L flasks each containing 750 mL of LB broth, both supplemented with 100  $\mu\text{g}/\text{mL}$  ampicillin. Cultures were incubated at 37 °C while being shaken at 300 rpm until they reached an OD<sub>600</sub> of 0.5. *B. subtilis* TrxR expression was induced with 0.2 mM IPTG for 3 h at 30 °C and 300 rpm, while *B. subtilis* TrxA expression was induced with 8.76 mM L-lactose for 5 h at 30 °C at 150 rpm before cells were harvested by centrifugation at 6745g for 10 min. Cell pellets were stored at –20 °C until further use.

TrxA and TrxR containing His affinity tags were purified using a Ni<sup>2+</sup>-IMAC (immobilized metal affinity chromatography) column according to the procedure described below. Cell pellets were resuspended in 1:5 weight:volume ratio of buffer A and lysed with an Emulsiflex C5 high-pressure homogenizer (Avestin) at 10000–15000 psi. Lysed cell debris was separated from the crude extract solution by centrifugation at 12800g for 20 min. The clear supernatant was loaded onto a 5 mL Ni<sup>2+</sup>-IMAC column (GE Healthcare) pre-equilibrated with buffer A. The column was washed with buffer A, and proteins were eluted in a stepwise gradient of buffer A containing 25, 50, and 250 mM imidazole using a fast protein liquid chromatography (FPLC) system (AktaPurifier, GE Healthcare). Fractions containing TrxR were eluted as a single peak with 250 mM imidazole and displayed a bright yellow color corresponding to the presence of the expected oxidized FAD cofactor associated with the enzyme. Fractions containing TrxA were eluted with 250 mM imidazole displaying coloration characteristic of Fe–S proteins. Sodium dodecyl sulfate–polyacrylamide gel electrophoresis analysis was performed to evaluate the purity of the eluted fractions. TrxR was reduced with 2 mM DTT, and both TrxA and TrxR were dialyzed against at least 10 volume equivalents of buffer A overnight at 4 °C and then pelleted in liquid nitrogen prior to being stored at –80 °C until further use. *B. subtilis* cysteine desulfurases (SufS and YrvO) and sulfur acceptor proteins (SufU, MnmA, and YrkF) were expressed and purified as described previously.<sup>11,13,61</sup>

**TrxA Assays.** All reactions were performed anaerobically in the glovebox and carried out with capped anaerobic quartz cuvettes (Starna). Solutions of NADPH, insulin, GSSG, DTNB, and L-cysteine were freshly prepared in degassed 50 mM potassium phosphate buffer in the anaerobic chamber.

Table 1. Kinetic Parameters for the *B. subtilis* Trx System (top) and Orthologous Systems

	substrate	$K_{\text{cat}}$ ( $\text{s}^{-1}$ ) <sup>a</sup>	$K_{\text{M}}$ ( $\mu\text{M}$ )	ref
<i>B. subtilis</i> TrxR	TrxA		4.22 ± 0.58	Figure S3
	NADPH	6.5 ± 0.6 <sup>b</sup>	134 ± 31	
<i>Bacillus anthracis</i> TrxR	Trx1	13.5 ± 0.15	8.41 ± 0.32	65
	Trx2		19.2 ± 1.39	
	NrdH		85.5 ± 5.98	
<i>E. coli</i> TrxR	Trx1	33.5 ± 2.3	3.68 ± 0.63	69
	NADPH		2.69 ± 0.59	
<i>Helicobacter pylori</i> TrxR	Trx1	75	22.6	66
	NADPH		6.1	
	substrate	$K_{\text{cat}}$ ( $\text{s}^{-1}$ ) <sup>a</sup>	$K_{\text{M app}}$ ( $\mu\text{M}$ )	ref
<i>B. subtilis</i> TrxR–TrxA	insulin	2.2 ± 0.085 <sup>c</sup>	96 ± 14.1	Figure S4
	GSSG	2.63 ± 0.089 <sup>c</sup>	990 ± 110	
	DTNB	2.15 ± 0.132 <sup>c</sup>	36 ± 15.5	
	SufU-SSH	3.75 ± 0.47 <sup>c</sup>	22.8 ± 7.7	
<i>B. anthracis</i> TrxR–Trx1	RNR	0.149 ± 0.002 <sup>d</sup>	0.54 ± 0.05	65
<i>E. coli</i> TrxR–Trx1	insulin	8.7	11	70
	GSSG		400 <sup>e</sup>	
<i>Staphylococcus aureus</i> TrxR–TrxA	CstA <sup>RhodTusA</sup>	8.15 ± 2.16	9 ± 2.3 <sup>f</sup>	71, 72
	CstA <sup>Rhod</sup> -SSH		530.8 ± 82	
	PykA-SSH		39 ± 15	

<sup>a</sup>Turnover number normalized by the FAD occupancy of as-isolated TrxR. <sup>b</sup> $K_{\text{cat app}}$  determined using 15  $\mu\text{M}$  TrxA and 5.8 nM TrxR-FAD. <sup>c</sup> $K_{\text{cat app}}$  determined using 20  $\mu\text{M}$  TrxA and 51 nM TrxR-FAD. <sup>d</sup>The turnover number is dNDP turnover by RNR. Each turnover of RNR requires one turnover of the Trx system. <sup>e</sup>Estimated from ref 43. <sup>f</sup>Disulfide substrate.

Each reaction was initiated by adding the substrate insulin, GSSG, DTNB, or cysteine with a syringe. Unless otherwise indicated, 1 mL reactions were performed with varying concentrations of each substrate in 50 mM phosphate buffer containing 51 nM TrxR-FAD, 20  $\mu\text{M}$  TrxA, 0.4 mM NADPH, and 0.25 mM EDTA. NADPH oxidation was monitored by absorbance at 340 nm in a Cary 50 spectrophotometer in continuum mode, and the negative slopes of absorbance per minute were converted to nanomoles of NADPH oxidized per minute using the molar absorption coefficient (6.22  $\text{mM}^{-1} \text{cm}^{-1}$ ). The reduction of DTNB by Trx was monitored at 412 nm, and a standard curve of TNB was generated upon reduction of the substrate with DTT under the same buffer conditions.

**Persulfide Reduction Assay.** Protein persulfide formation was accomplished by cysteine desulfurase reactions in the presence and absence of their respective sulfur acceptors. Unless otherwise indicated, reactions were conducted in 1 mL volumes containing 50 mM potassium phosphate buffer (pH 8), initiated by the addition of 0.5 mM L-cysteine. The reduction of persulfide intermediates formed and residing on either the cysteine desulfurase or the sulfur acceptor was achieved through the addition of either 2 mM DTT, 2 mM TCEP, or the Trx system, which included 20  $\mu\text{M}$  TrxA, 51 nM TrxR-FAD, 0.4 mM NADPH, and 0.25 mM EDTA. The competency of each reductant to act on the protein persulfide intermediates was determined through quantification of sulfide or alanine produced in these reactions over time using the methylene blue or Ala-NDA assay, respectively.<sup>21</sup> The rate of sulfide or Ala formation was calculated using freshly prepared standard curves, and cysteine desulfurase activity was determined using the slopes from at least four time points. For NADPH oxidation/persulfide reduction coupled assays, 50  $\mu\text{L}$  reaction aliquots were taken at various time points for sulfide quantification using the methylene blue assay.

**In Vitro Cluster Reconstitution on Apo-TrxA.** Cluster reconstitution reactions (5 mL) were conducted in an anaerobic chamber (Coy) equilibrated with 1.5%  $\text{H}_2$  and balanced with  $\text{N}_2$  gas. Reaction mixtures containing 100  $\mu\text{M}$  *B. subtilis* apo-TrxA, 0.5  $\mu\text{M}$  SufS, 5  $\mu\text{M}$  SufU, 1.2 mM  $\text{Fe}(\text{NH}_4)_2(\text{SO}_4)_2$ , 0.5 mM L-cysteine, and 1 mM DTT in 25 mM Tris-HCl (pH 8) were incubated for 2 h. Following incubation, reaction mixtures were loaded onto a 1 mL  $\text{Ni}^{2+}$ -IMAC column (GE Healthcare) pre-equilibrated with buffer B [25 mM Tris-HCl (pH 8) and 0.15 M NaCl]. To ensure removal of additional reaction components, the column was washed with at least 3 column volumes of buffer B containing 50 mM imidazole, and subsequently, holo-TrxA was eluted with buffer B containing 250 mM imidazole. Control experiments including the same reaction components in the absence of TrxA showed no Fe–S clusters in the elution fraction from the  $\text{Ni}^{2+}$ -IMAC column, a finding similar to that reported previously.<sup>62</sup>

**Size Exclusion Analysis.** The oligomeric states of apo-TrxA and reconstituted TrxA were determined using a 24 mL Superose 10/300 gel filtration column (GE Healthcare) connected to an FPLC system (AktaPurifier, GE Healthcare) and pre-equilibrated with buffer B at a flow rate of 0.4 mL/min. Protein standards were employed to generate a calibration curve and thus to estimate the oligomeric size of TrxA in its apo- and holo-reconstituted forms.

**Fe and S Analyses.** Iron determination was performed through complex formation with 2',2'-dipyridyl. Samples (400  $\mu\text{L}$ ) were mixed with 100  $\mu\text{L}$  of 2 N HCl and heated at 80 °C for 10 min. Subsequently, 500  $\mu\text{L}$  of  $\text{H}_2\text{O}$ , 50  $\mu\text{L}$  of 5 N NaOH, 100  $\mu\text{L}$  of 10% hydroxylamine, 100  $\mu\text{L}$  of 20 mM 2',2'-dipyridyl, and 50  $\mu\text{L}$  of 1 M Tris (pH 8) were added. Samples were centrifuged for 10 min, and  $\text{Abs}_{520}$ , resulting from the dipyridyl–ferrous complex, was evaluated in 200  $\mu\text{L}$  aliquots of the supernatant. The iron concentration in each sample was determined by comparison to a standard curve using fixed

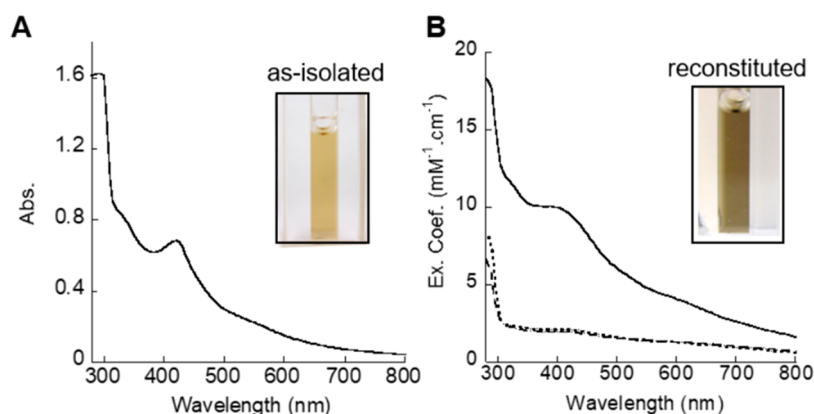


**Figure 1.** *B. subtilis* TrxA is able to coordinate Fe–S species. (A) UV–vis absorption spectrum of recombinant TrxA as isolated from *E. coli* under anoxic conditions. (B) UV–vis absorption spectra of TrxA (solid line), TrxA C29A (dashed line), and TrxA C32A (dotted line) after Fe–S cluster reconstitution and purification. The insets show the pictures of the wild type TrxA solution as isolated (A) and after reconstitution (B). Similar spectra for as-isolated and reconstituted samples were observed in more than five independent experiments.

concentrations of  $\text{Fe}(\text{NH}_4)_2(\text{SO}_4)_2$ . Acid-labile sulfur was measured using the methylene blue method.<sup>63</sup>

## RESULTS

**Isolation of TrxR and TrxA in Their Apo and Fe–S-Bound Forms.** The investigation of the thioredoxin system's reactivity was initiated by the expression and isolation of each individual component. As expected, TrxR displayed a yellow color attributed to the flavin adenine dinucleotide (FAD) cofactor associated with the enzyme (Figure S2). On the basis of the molar absorptivity of FAD ( $\sum_{456} = 11.3 \text{ mM}^{-1} \text{ cm}^{-1}$ ),<sup>64</sup> the as-isolated TrxR contained 34.6% cofactor occupancy, and addition of FAD to the purified protein increased its activity only marginally by 20% (from 1.33 to 1.60  $\mu\text{mol}$  of NADPH oxidized  $\text{min}^{-1} \text{ mg}^{-1}$ ). The substoichiometric occupancy of the cofactor has also been reported for TrxR orthologous enzymes.<sup>65–68</sup> Incubation of TrxR with 5 molar equivalents of NADPH or NADH led to a change in the absorbance spectrum, consistent with the reduction of dinucleotide and consequent formation of FADH<sub>2</sub>. Although NADH was able to reduce TrxR, the specific activity of the enzyme in the presence of the dinucleotide reductant (0.4  $\mu\text{M}$ ) was 5 times lower than that of reactions employing NADPH (0.26  $\mu\text{mol}$  of NADH oxidized  $\text{min}^{-1} \text{ mg}^{-1}$  vs 1.33  $\mu\text{mol}$  of NADPH oxidized  $\text{min}^{-1} \text{ mg}^{-1}$  under the same conditions). Kinetic characterization of TrxR reported here utilized NADPH as the electron donor and TrxR-FAD (as isolated) in an anoxic variation of the commonly used insulin assay<sup>43</sup> to minimize background flavin oxidation from environmental oxygen. Considering the FAD occupancy of the as-isolated TrxR, the kinetic parameters of TrxR for thioredoxin were comparable to those reported for orthologous enzymes (Figure S3 and Table 1).

As-isolated TrxA displayed an unexpected brown-reddish color. The UV–vis absorption spectrum of TrxA isolated under anoxic conditions showed features characteristic of Fe–S cluster-containing proteins (Figure 1A). Metal species associated with TrxA were present at substoichiometric ratios of Fe and acid-labile sulfide to TrxA and varied with growth condition and purification preparation (0.1–0.25:0.1–0.2:1 Fe:S:TrxA). Fe–S species associated with TrxA were prone to degradation upon being exposed to oxygen, which is evidenced by the loss of metal content during purification and buffer exchange outside of the anaerobic chamber. The ability of

TrxA to coordinate Fe–S species at stoichiometric levels was observed upon *in vitro* reconstitution of TrxA, isolated through  $\text{Ni}^{2+}$ -IMAC chromatography. Holo-TrxA, containing  $2.11 \pm 0.05$  Fe and  $1.75 \pm 0.25$  S, displayed absorption features characteristic of Fe–S cluster-bound proteins (Figure 1B). The cluster associated with the protein was readily labile and remains to be characterized by additional spectroscopic approaches. Size exclusion chromatography demonstrated a change in oligomeric state upon reconstitution of holo-TrxA. Apo-TrxA (molecular weight of 11.4 kDa) exhibited a calculated molecular weight of 16.7 kDa, similar to the size of a monomer. Alternatively, the elution volume for a single distinct peak containing holo-reconstituted TrxA corresponded to an apparent molecular weight of 67 kDa, suggesting formation of a tetramer, or another oligomeric state. The activity of the three forms of TrxA (as-isolated and apo- and holo-reconstituted) showed that the ligation of Fe–S species to the protein resulted in the loss of its standard dithiol-reductase activity (Figure 2). Whether the accumulation of Fe–S species leading to a change in quaternary structure and TrxA inactivation represents an artifact of the expression system or a bona fide mechanism of Trx system regulation is not known at this point and will be investigated in future studies. For the remaining experiments reported in this study, the aerobically purified apo-TrxA was used as the source of redox active TrxA.

### Reactivity of TrxA toward Disulfide Substrates.

Thioredoxin proteins are well-characterized with regard to their associated disulfide reductase activities as cosubstrates of thioredoxin reductase. The oxidoreductase activity of thioredoxins depends on two strictly conserved cysteine residues. One is the catalytic residue, responsible for initiating the reaction through a nucleophilic attack on the disulfide bond of the substrate and concomitantly forming a covalent disulfide intermediate with the substrate. The reaction is completed by the second Cys residue, termed as the resolving cysteine, which releases the reduced product upon re-formation of the thioredoxin disulfide bond with the catalytic Cys residue.<sup>45</sup> *B. subtilis* TrxA contains only two Cys residues, C29 and C32, proposed to act as the catalytic and resolving residues, respectively.<sup>73</sup> As expected, substitution of either cysteine residue with an alanine led to a loss of activity (Figure 2). In addition, both TrxA C29A and C32A variants also lost the ability to coordinate Fe–S species, indicating that both active

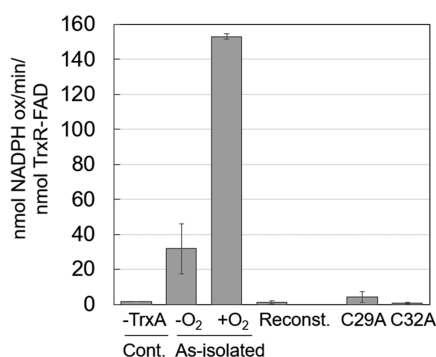


**Figure 2.** Activity profile of wild type TrxA and its variants. The activity of TrxA was determined in the presence of 51 nM TrxR-FAD, 0.4 mM NADPH, and 3 mM GSSG in 50 mM potassium phosphate and 0.25 mM EDTA (pH 7). Control experiments were performed in the absence of TrxA. The as-isolated enzyme under anoxic conditions ( $-O_2$ ) showed reduced activity when compared to that of the sample isolated under aerobic conditions ( $+O_2$ ), whereas TrxA after Fe-S cluster reconstitution and IMAC purification (Reconst.) showed no activity. Control experiments carried out with equivalent concentrations of imidazole in the reaction buffer showed no inhibition (data not shown). Likewise, aerobically as-isolated TrxA variants containing substitutions of either active site cysteine (C29A or C32A) also showed no activity.

site residues serve as potential cluster ligands (Figure 1B). Kinetic characterization of *B. subtilis* TrxA reactivity toward standard disulfide substrates was determined for oxidized glutathione (GSSG), S,S-dithiobis(2-nitrobenzoic acid) (DTNB), and insulin (Table 1 and Figure S4). Similar to that of the *E. coli* TrxR-Trx1 reaction,<sup>74</sup> maximal activity for the *B. subtilis* enzyme was achieved in phosphate buffer at pH 8 [ $187 \mu\text{mol}$  of NADPH oxidized  $\text{min}^{-1}$  ( $\mu\text{mol}$  of TrxR-FAD) $^{-1}$ ] and reduced to 30% in reactions performed in Tris or HEPES buffer [ $45$  or  $50 \mu\text{mol}$  of NADPH oxidized  $\text{min}^{-1}$  ( $\mu\text{mol}$  of TrxR-FAD) $^{-1}$ , respectively]. The disulfide substrate saturation profile demonstrated that TrxA was less efficient in reducing disulfides than the *E. coli* Trx1 enzyme.<sup>43</sup> Nevertheless, the *B. subtilis* ortholog displayed considerable reactivity toward disulfide substrates.

**Reactivity of TrxA toward Persulfide Protein Substrates.** While the reactivity of bacterial Trx proteins toward disulfides has been well-documented, their participation in biosynthetic pathways involving the formation and transfer of persulfidic sulfur has not been fully explored.

Recent research points to the involvement of Trx proteins in maintaining overall levels of persulfides in eukaryotic cells through reduction of low-molecular weight persulfides (Cys-SSH and GSSH) as well as protein persulfides (HSA-SSH and TSTD1-SSH).<sup>75–77</sup> In recent reports, the reactivity of *Staphylococcus aureus* TrxA toward persulfides has also been pointed out as a relevant mediator in H<sub>2</sub>S signaling.<sup>71,72</sup> The chemical similarities between persulfides and disulfides, combined with the involvement of the Trx system in the maintenance of cellular persulfide and sulfide levels, prompted us to investigate if Trx proteins were suitable components of biosynthetic schemes requiring reduction of persulfide intermediates formed during catalysis.

In previous work, we have characterized the mechanism of the Cys:SufU sulfurtransferase activity of *B. subtilis* SufS.<sup>11,62</sup> The proposed catalytic scheme for this reaction involves the mandatory formation of a persulfide enzyme intermediate

(SufS-SSH) and a subsequent persulfide sulfur transfer event promoted by the nucleophilic attack of a deprotonated Cys thiol of the sulfur acceptor substrate, zinc-bound SufU. *In vitro* reactions probing the SufS-SufU kinetic profile of persulfide formation and reduction included the presence of artificial reductants dithiothreitol (DTT) and tris(2-carboxyethyl)-phosphine (TCEP).<sup>62</sup> Both of these reductants are capable of reducing the persulfide bond on SufU by liberating sulfide ( $S^{2-}$ ), resetting this sulfur acceptor to interact with SufS in the subsequent catalytic cycle. Here, reaction rates monitored by the formation of  $S^{2-}$  were determined in the presence of the Trx system and compared to rates determined in the presence of DTT (Figure 3A). These analyses showed that, like artificial

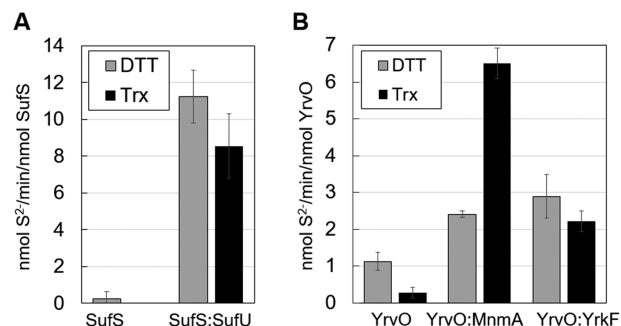


**Figure 3.** The Trx system is catalytically competent in reducing persulfide species formed on *B. subtilis* sulfur acceptors. (A) The rate of sulfide formation is shown upon the reduction of protein persulfides formed in 1 mL reaction mixtures containing  $0.22 \mu\text{M}$  SufS and  $0.5 \text{ mM}$  Cys in the absence or presence of  $2.2 \mu\text{M}$  sulfur acceptor Zn-bound SufU. (B) Rate of sulfide formation upon reduction of protein persulfides formed in 1 mL reaction mixtures containing  $1.2 \mu\text{M}$  YrvO and  $0.5 \text{ mM}$  Cys in the absence or presence of sulfur acceptor MnmA ( $12 \mu\text{M}$  in the presence of  $1 \text{ mM}$  ATP and  $5 \text{ mM}$  MgCl<sub>2</sub>) or YrkF ( $7.2 \mu\text{M}$ ). Reactions were performed in  $50 \text{ mM}$  phosphate buffer (pH 8) using  $2 \text{ mM}$  DTT (gray bars) as a reductant or in the presence of the Trx system including  $51 \text{ nM}$  TrxR-FAD,  $20 \mu\text{M}$  TrxA,  $0.25 \text{ mM}$  EDTA, and  $0.4 \text{ mM}$  NADPH (black bars). Reactions performed in the absence of either DTT or TrxA showed no production of sulfide over time (data not shown).

reductants, a physiological reductant is competent in reducing persulfides formed within the sulfur acceptor SufU but not reactive toward transient persulfides residing within SufS.

Likewise, the Trx system was equally competent in serving as a reductant in reactions performed by the *B. subtilis* cysteine desulfurase YrvO and its sulfur acceptors, MnmA and YrkF (Figure 3B). In the absence of either sulfur acceptor protein, the Trx system was unable to promote catalytic turnover of YrvO at a rate similar to that observed with the artificial reductant DTT. However, comparison between the activity enhancement achieved by YrvO sulfur acceptor proteins with either reductant revealed that the Trx system was far more effective than DTT in reducing persulfides within the sulfur acceptor protein. Specifically, with DTT as the reductant, the presence of MnmA facilitated a modest 2-fold enhancement of YrvO activity, whereas in reaction mixtures reduced by the thioredoxin system, MnmA enhanced YrvO activity by 24-fold. Likewise, the enhancement of sulfide production achieved in the presence of YrkF, the other sulfur acceptor protein of YrvO, also varied depending on the reductant used. Similar to MnmA, YrkF enabled a mere 2-fold increase in YrvO's basal activity under DTT-reducing conditions, while an 8-fold

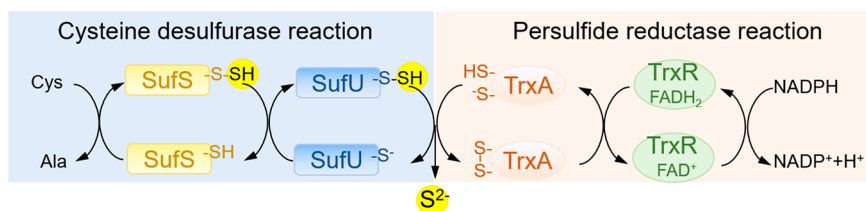


**Figure 4.** Kinetic scheme of SufS:SufU sulfurtransferase and Trx reductase coupled reactions. Diagram of the proposed kinetic scheme involving the Cys:SufU sulfurtransferase reaction of SufS (blue-shaded area) coupled with the persulfide reductase reaction of the Trx system (salmon-shaded area). The coupled reaction involves the NADPH-dependent reduction of SufU persulfide intermediates formed in the SufS reaction by TrxA and TrxR, releasing sulfide as a final product.

enhancement was observed in reaction mixtures reduced by the thioredoxin system. Collectively, the results shown here demonstrate that the reactivity of *B. subtilis* cysteine desulfurases is restricted to sulfur acceptor proteins and not susceptible to the action of general thiol-oxidoreductases. These observations are in agreement with both our initial kinetic analyses of cysteine desulfurases and our working model that these pathways involve a mandatory persulfide sulfur transfer event from the cysteine desulfurase to the sulfur acceptor prior to persulfide reduction.

**TrxR–TrxA and SufS–SufU Display Coupled Reaction Schemes.** The involvement of the Trx system in reactions forming persulfide intermediates suggests that the availability of reduced TrxA may limit the rate of sulfur mobilization by cysteine desulfurases. Likewise, the transient accumulation of protein persulfides, serving as substrates of TrxA, may also impact the rate of NADPH consumption promoted by the TrxR–TrxA reaction. Thus, we proposed that the occurrence of coupled kinetic schemes links the rate of NADPH consumption to the rate of sulfide production and vice versa (Figure 4). Therefore, this hypothesis was tested in reaction assays containing varying concentrations of the Trx system with constant concentrations of the SufS–SufU pair (Figure 5A). Under these conditions, the rate of sulfide production exhibited a hyperbolic response with a calculated  $V_{\max}$  of  $22.5 \pm 1.5 \text{ nmol of S}^{2-} \text{ min}^{-1} (\text{nmol of SufS})^{-1}$ , which is higher than the activity for this enzyme in the presence of 2 mM DTT [ $11.25 \pm 6.3 \text{ nmol of S}^{2-} \text{ min}^{-1} (\text{nmol of SufS})^{-1}$ ] but close to the activity values of the enzyme in the presence of 2 mM TCEP [ $30 \pm 6.3 \text{ nmol of Ala min}^{-1} (\text{nmol of SufS})^{-1}$ ]. The effect of reductants on the activity of the SufS–SufU reaction supports previous findings that the overall rate is limited by the last reaction step, the reduction of the transient persulfide residing within the sulfur acceptor substrate SufU.<sup>62</sup> Furthermore, increasing concentrations of the Trx system led to acceleration of this step through an increased flux of reductant, thereby accelerating the overall reaction.

The occurrence of a coupled reaction scheme was also demonstrated in the reciprocal experiment in which reactions with fixed concentrations of the Trx system were performed with varying concentrations of the SufS–SufU pair (Figure 5B). In the SufS–SufU saturation plot, the maximum activity reached by the Trx system was similar to those determined for disulfide substrates (Figure 5B). Interestingly, the calculated  $K_M \text{ SufU}$  of the persulfurated substrate (provided by the SufS–SufU reaction in the presence of cysteine) was  $22.85 \pm 7.7 \mu\text{M}$ . This value is lower than the  $K_M$  estimated for insulin or GSSG, demonstrating that the *B. subtilis* Trx system has a higher catalytic efficiency upon reduction of persulfides that accumulated within SufU. Analysis of sulfide production in

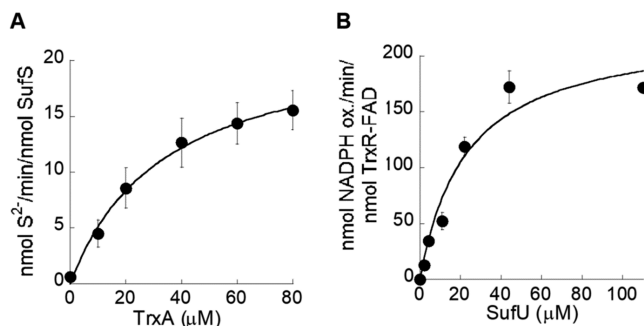


**Figure 5.** Activity profile of SufS:SufU and Trx system coupled reactions. (A) Activity profile of the SufS:SufU reaction in the presence of increasing concentrations of the Trx system. The rates of sulfide production were determined in 1 mL reaction mixtures using  $0.22 \mu\text{M}$  SufS and  $2.2 \mu\text{M}$  SufU in the presence of  $0.25 \text{ mM}$  EDTA,  $0.4 \text{ mM}$  NADPH,  $0.5 \text{ mM}$  Cys, and increasing concentrations of both TrxA and TrxR in  $50 \text{ mM}$  phosphate buffer (pH 8). The ratio of TrxA to TrxR-FAD was kept constant at 392:1. The line is the best fit of the Michaelis–Menten equation providing a  $V_{\max}$  of  $22.5 \pm 1.5 \text{ nmol of S}^{2-} \text{ min}^{-1} (\text{nmol of SufS})^{-1}$  ( $K_{\text{cat SufS}}$  of  $0.375 \text{ s}^{-1}$ ) and a  $K_M \text{ TrxA}$  of  $34 \pm 5.4 \mu\text{M}$ . (B) Activity profile of the Trx system in the presence of increasing concentrations of SufS:SufU. The rate of NADPH oxidation was determined in 1 mL reaction mixtures containing  $20 \mu\text{M}$  TrxA and  $51 \text{ nM}$  TrxR-FAD,  $0.25 \text{ mM}$  EDTA,  $0.4 \text{ mM}$  NADPH,  $0.5 \text{ mM}$  Cys, and increasing concentrations of both SufS and SufU in  $50 \text{ mM}$  phosphate buffer (pH 8). The ratio of SufU to SufS was kept constant at 10:1. The line is the best fit of the Michaelis–Menten equation providing a  $V_{\max}$  of  $225 \pm 28 \text{ nmol of NADPH oxidized min}^{-1} (\text{nmol of TrxR-FAD})^{-1}$  ( $K_{\text{cat TrxR-FAD}}$  of  $3.75 \text{ s}^{-1}$ ) and a  $K_M \text{ SufU}$  of  $22.85 \pm 7.7 \mu\text{M}$ .

reaction mixtures containing increasing concentrations of SufS–SufU showed that at high concentrations of SufS–SufU, the rate of the reaction is limited by the turnover rate of the TrxR–TrxA pair (Figure 6), whereas reactions performed with an excess of the artificial reducing agent (2 mM DTT) displayed a linear concentration-dependent activity. Cumulatively, these kinetic analyses reveal contributions to the modulation of cysteine desulfurase reactivity by physiological factors not previously implicated in such reactions. It is well-known that the overall reaction involving the conversion of Cys to Ala and  $\text{S}^{2-}$  is affected by the cellular concentration of the substrate Cys. Our findings demonstrate that in addition to the concentration of the Cys substrate, this reaction is also affected by reducing equivalents provided by the Trx system as well as the availability of all four proteins.

**Inactivation of the Thioredoxin System Affects the Activity of Fe–S Enzymes.** Biochemical defects associated with the inactivation of TrxR or TrxA mirrored the defects identified for inactivation of *sufU* in Fe–S cluster biogenesis.<sup>78</sup>

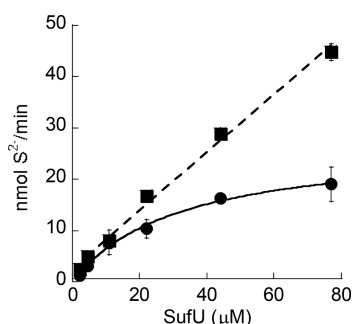


**Figure 6.** Rate of production of sulfide from the Cys:SufU sulfurtransferase reaction that depends on the availability of the reductant system. The rate of sulfide production was determined using increasing concentrations of SufS and SufU while keeping a constant ratio of 1:10 using 2 mM DTT (squares) or the Trx system (circles). Reactions in 50 mM phosphate buffer (pH 8) (1 mL) were initiated upon addition of 0.5 mM Cys. When the Trx system was used as a reductant, reactions included 20  $\mu$ M TrxA, 51 nM TrxR-FAD, 0.25 mM EDTA, and 0.4 mM NADPH. The concentration-dependent profile of DTT-containing reactions exhibited a linear response ( $\nu = 0.56[\text{SufU}] + 2.5$ ;  $R^2 = 0.98$ ), whereas Trx-containing reactions showed a hyperbolic response [ $\nu = (27[\text{SufU}]) / (32 + [\text{SufU}])$ ];  $R^2 = 0.98$ ].

Both SufU and SufS are proposed to be involved in the initial steps of Fe–S cluster biogenesis through mobilization of sulfur from Cys. Inactivation of *B. subtilis* *sufU* resulted in reduced activity of the Fe–S enzymes, aconitase and succinate dehydrogenase (25% and 75% of wild type levels, respectively).<sup>78</sup> Therefore, the reactivity of the Trx system toward reactions performed by SufS–SufU led us to interrogate the possible involvement of both TrxA and TrxR in *B. subtilis* Fe–S metabolism. In this proposed model, if the activity of the Trx system affects the activity of the Suf system *in vivo*, then inactivation of either Trx component would likewise impact the maturation of Fe–S enzymes. To test this hypothesis, the activity levels of the Fe–S enzymes aconitase (ACN), isopropylmalate isomerase (LeuCD), and glutamine:2-oxoglutarate amidotransferase (GOGAT) were quantified in cell extracts impaired for either component of the Trx system. Previous studies targeting downregulation of *trxA* showed alternate patterns of expression upon *trxA* depletion. However, none of the genes encoding enzymes tested in this experiment were included in the extended list of genes with differential expression patterns.<sup>52</sup>

*In vivo* inactivation of TrxR was achieved by the addition of ebselen to *B. subtilis* cultures at concentrations that moderately inhibited growth but were not lethal (Figure S5). Ebselen is a potent inhibitor of TrxR found in Gram-positive species like *Mycobacterium tuberculosis*, *S. aureus*, and *Bacillus anthracis*.<sup>79,80</sup> *In vitro* inhibition assays showed that ebselen displayed a low IC<sub>50</sub> against TrxR (32  $\pm$  0.11 nM) (Figure S6), and therefore, the concentration used for *in vivo* inhibition (0.51  $\mu$ M) was most likely sufficient. Interestingly, extracts of cultures exposed to ebselen displayed significant impairment of the activity of both Fe–S enzymes LeuCD and GOGAT and modest impairment of the activity of the Fe–S enzyme ACN (Figure 7A). It is possible that ebselen can alter the expression of these enzymes; however, the activity of malate dehydrogenase, an enzyme that does not contain Fe–S clusters, was unaffected. In addition, the activity of mononuclear iron-dependent enzymes, threonine dehydrogenase (TDH) and quercetin 2,3-dioxyge-

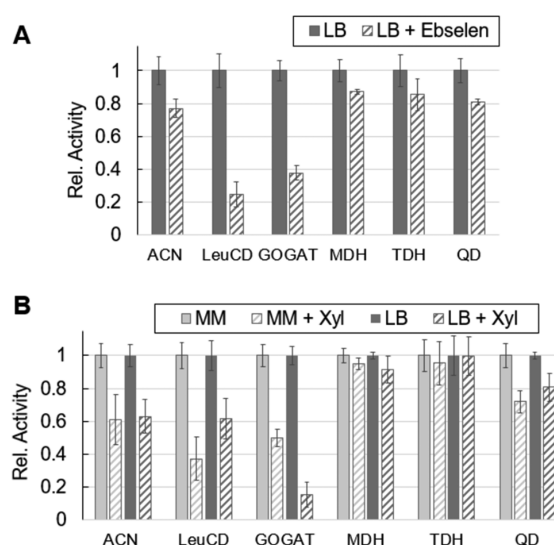


**Figure 7.** Inactivation of the Trx system affects the activity of Fe–S enzymes. Cell extracts prepared anoxically were tested for the activity of Fe–S enzymes aconitase (ACN), isopropylmalate isomerase (LeuCD), and glutamine:2-oxoglutarate amidotransferase (GOGAT), and these activities were compared to the activities of non-Fe–S enzymes malate dehydrogenase (MDH) and iron-only threonine dehydrogenase (TDH) and quercetin 2,3-dioxygenase (QD). (A) The activities of these enzymes were determined for the *B. subtilis* PS832 strain cultured in LB in the absence and presence of the thioredoxin reductase inhibitor ebselen. The relative ACN, LeuCD, GOGAT, MDH, TDH, and QD activities were calculated from extracts of cells cultured in the absence of the inhibitor (68, 17, 35, 1309, 9.4, and 11 nmol min<sup>-1</sup> mg<sup>-1</sup>, respectively). (B) The activities of these enzymes were determined for the *B. subtilis* BEC28500 strain cultured in minimal medium (MM, Spizizen) and LB in the absence and presence of 1% xylose, which induced CRISPR/dCas9 inactivation of *trxA*. The relative ACN, LeuCD, GOGAT, MDH, TDH, and QD activities were calculated from extracts of cells cultured in MM (64, 20, 39, 1555, 13, and 13 nmol min<sup>-1</sup> mg<sup>-1</sup>, respectively) and in LB (71, 14, 35, 1554, 12, and 10 nmol min<sup>-1</sup> mg<sup>-1</sup>, respectively) in the absence of xylose. The reported averages and associated standard deviation were based on data acquired from at least three independent experiments.

nase (QD), was also evaluated. Ebselen treatment of *B. subtilis* cultures had a minor effect on the activity of these enzymes, but the extent of inhibition was less than that imposed on Fe–S-dependent enzymes (Figure 7).

Like *trxR*, *trxA* is also an essential gene in *B. subtilis*, thus making standard genetic approaches for direct gene inactivation unviable. However, Peters et al. reported the use of the CRISPR (clustered regularly interspaced short palindromic repeats) interference (CRISPRi) approach, in which single guided RNA sequences direct deactivated nuclease Cas9 (*dCas9*) to halt transcription of targeted genes.<sup>53</sup> Using this CRISPRi approach, the *B. subtilis* BEC28500 strain was constructed to allow for the inactivation of *trxA* transcription upon induction with 1% xylose.<sup>53</sup> Because of the essential role of TrxA in *B. subtilis*, the BEC28500 strain cultured in the presence of xylose exhibited reduced growth (Figure S5). To monitor the impact of TrxA on Fe–S enzyme activity, we quantified the activity of Fe–S enzymes from cell extracts of *B. subtilis* BEC28500 cultured in minimal medium (MM) and in rich medium (LB), in the presence and absence of xylose. Similar to inactivation of TrxR, a reduced level of expression of TrxA also led to a loss of the activity of Fe–S



enzymes, supporting the notion that both components of the Trx system are involved in Fe–S metabolism (Figure 7B).

## DISCUSSION

The biosynthesis of sulfur-containing cofactors, including Fe–S clusters, involves the formation, transfer, and reduction of protein persulfides.<sup>4</sup> Here, we have shown that the *B. subtilis* thioredoxin system, in addition to displaying standard activity toward disulfide substrates, is a competent physiological reductant of protein persulfides formed as products of upstream cysteine desulfurase reactions.<sup>21</sup> The activation of sulfur by cysteine desulfurases involves the initial mandatory formation of a transient persulfide on the active site cysteine residue of the cysteine desulfurase, followed by a persulfide sulfur transfer step to the subsequent sulfur acceptor protein. The thioredoxin system was an effective reductant of persulfides formed within sulfur acceptor proteins but showed limited to no reactivity toward transient persulfides formed on the cysteine desulfurases during their catalytic cycle. This reactivity profile is distinct from that observed for reactions performed in the presence of artificial reducing agents. However, the profile is in agreement with *in vivo* data demonstrating the indispensable requirement of sulfur acceptor proteins in mediating sulfur trafficking from cysteine desulfurases during thio-cofactor biosynthesis.<sup>13,78,81</sup>

The involvement of the Trx system as a physiological persulfide reductant was investigated here in reactions performed by two *B. subtilis* cysteine desulfurases, SufS and YrvO. Like the components of the Trx system, both cysteine desulfurases, along with their characterized sulfur acceptors, SufU and MnmA, are essential enzymes in *B. subtilis*. Previously, we have identified MnmA and YrkF as competent sulfur acceptors of YrvO.<sup>61</sup> The essentiality of YrvO, along with MnmA, is attributed to their sequential roles in sulfur activation and insertion into the U34 position of tRNA<sup>Glu</sup>, tRNA<sup>Gln</sup>, and tRNA<sup>Lys</sup> to form the 2-thiouridine (s<sup>2</sup>U) tRNA modification.<sup>13</sup> In this pathway, MnmA performs two consecutive reactions: the adenylation of the C2 position of U34 tRNA and then the sulfur transfer via a persulfide intermediate from YrvO to form s<sup>2</sup>U. In reaction mixtures containing DTT, MnmA enhances the turnover rate of YrvO 2-fold, but only in the presence of ATP, suggesting that the ATP-bound form of the thiouridylase is the catalytically competent form of the sulfur acceptor, as described previously.<sup>13</sup> Here, we showed that the Trx system is an efficient reductant of persulfides formed on ATP-bound MnmA *in vitro*, enhancing the rate of sulfide production by 24-fold [from 0.26 to 6.35 nmol min<sup>-1</sup> (nmol of YrvO)<sup>-1</sup>]. Likewise, *in vitro* reactions performed with the sulfur acceptor, YrkF, displayed an 8-fold activity enhancement when the Trx system was used as a reductant. In the absence of either sulfur acceptor, the rate of sulfide production by YrvO was marginal, 4 times lower in reactions using the Trx system as the reductant [0.26 nmol min<sup>-1</sup> (nmol of YrvO)<sup>-1</sup>] than in those reduced by DTT [1.1 nmol min<sup>-1</sup> (nmol of YrvO)<sup>-1</sup>]. These results are aligned with the current model in which the sulfur transfer events initiated by cysteine desulfurases require the participation of a dedicated sulfur acceptor to abstract the persulfide sulfur on the cysteine desulfurase and direct it to downstream steps in the biosynthetic process. The lower efficiency of the Trx system, in comparison to that of DTT, in reducing persulfides within YrvO, combined with its higher

efficiency in persulfide reduction in the presence of YrvO sulfur acceptors, provides kinetic support for this model.

The reactivity of the Trx system toward persulfide intermediates formed within sulfur acceptors was also shown in reactions involving SufS and SufU. In *B. subtilis*, the SufCDSUB system is proposed to be the main pathway for the formation of Fe–S clusters.<sup>21</sup> The initial activation and transfer of sulfur include transient protein persulfides formed on Cys364 of SufS and Cys41 of SufU, acting as a zinc-dependent sulfurtransferase enzyme.<sup>11,62,81</sup> The subsequent steps leading to the synthesis of Fe–S clusters have not been experimentally defined but are proposed to include the SufBCD proteins serving as the site of cluster assembly prior to incorporation of the prebuilt Fe–S units into final protein acceptors. It is also anticipated that this pathway requires a physiological reducing agent to promote the reduction of persulfides (S<sup>0</sup>) to sulfide (S<sup>2-</sup>), the formal charge of sulfur adopted in Fe–S clusters. Kinetic analyses reported in this study showed that the thioredoxin system is an effective reductant of persulfides formed within SufU, but not SufS, confirming again the indispensable role of SufU as a dedicated sulfur acceptor of SufS. Furthermore, the turnover rate of the SufS reaction was dependent on the availability of reduced SufU, which in turn was dependent on the availability of reduced thioredoxin. Thus, under conditions of low redox flux, provided by low concentrations of the thioredoxin system in the reaction, the rate of sulfide production in cysteine desulfurase assays was limited by the rate of the thioredoxin system. Under conditions of high redox flux, reached through saturating concentrations of the Trx system, the rate of the SufSU reaction was higher than the maximum rate in reactions performed with DTT as the reductant. In this coupled kinetic scheme, the rate of NADPH consumption by TrxR was also dependent on the rate of persulfide formation by the SufSU system. The maximum rate of TrxR-mediated NADPH oxidation remained relatively constant, regardless of whether the substrates for TrxA were protein persulfides or disulfide species. The intracellular concentration of each component can be calculated from the reported copy number per cell from whole genome expression studies (SubtiWiki database)<sup>82</sup> and the average volume of a *B. subtilis* cell (4 fL).<sup>83</sup> In cells cultured in glucose minimal medium, the concentrations are estimated to be 0.45 μM SufS, 0.264 μM SufU, 3.12 μM TrxA, and 0.17 μM TrxR (Table S2). Although the expression profile of these proteins changes up to 10-fold across a variety of growth conditions, the relative concentration of SufS/TrxA/SufU is in agreement with the results of Western-blot analysis in cell extracts of *B. subtilis* (data not shown). Taken together, the *in vivo* reaction rates of both SufS and TrxR can be calculated from their reported kinetic constants and intracellular concentrations of each enzyme and substrate (Table S3). Using these parameters, it is estimated that cells growing in minimal medium generate 1.9 μM persulfurated SufU/min and 0.71 μM reduced thioredoxin/min. Thus, the similar rates of product formation indicate that fluctuations in cellular concentrations of any of these enzymes or substrates will impact the overall rate of persulfide formation and reduction. The dependency of *in vitro* reaction rates on both half-reactions, as presented in Figure 4, potentially links the availability of reducing equivalents, such as NADPH, to the production of S-containing cofactors. These cofactors are involved in a variety of cellular processes, including reactions in central metabolism that lead to the production of NAD(P)H equivalents.

Additional evidence of the involvement of the Trx system in Fe–S cluster metabolism was provided through quantification of Fe–S enzyme activities in *B. subtilis*. Inactivation of either TrxR or TrxA led to decreased levels of Fe–S enzymes ACN, LeuCD, and GOGAT, without major activity impairment of enzymes that do not contain Fe–S clusters. Importantly, while a prior study showed that cellular levels of TrxA impact the transcription of a variety of important genes in *B. subtilis*, genes encoding the Fe–S enzymes evaluated here were unaffected or expression was slightly enhanced by lower levels of TrxA.<sup>52</sup> Thus, inactivation of the Trx system recapitulated the reported effects of Suf system inactivation in *B. subtilis*. *In vitro* kinetic analyses reported in this study point to the reactivity of the Trx system toward persulfides formed within SufU. Interestingly, a recent report showed the association of the thioredoxin-like TrxP and SufB in disulfide proteomic profiling studies in *S. aureus*, suggesting once again the association of the Suf and Trx systems in Fe–S cluster biogenesis.<sup>72</sup> While this report demonstrates the reactivity of TrxA toward persulfides formed within SufU, the involvement of TrxA in subsequent steps of the cluster synthesis process should not be discarded at this point. It is also expected that TrxA, through its standard disulfide reductase activity, may be reactive toward cysteine residues serving as ligands of Fe–S clusters within final acceptor proteins. Parallel evidence linking the involvement of the thioredoxin system in Fe–S cluster biogenesis has been recently provided by biochemical analysis of yeast cells depleted of thioredoxin systems. Inactivation of cytosolic thioredoxin led to impairment of Fe–S enzymes with defects attributed to Fe–S cluster biosynthetic components present in the cytosol. Interestingly, inactivation of mitochondrial thioredoxin did not impair the synthesis of Fe–S clusters by the Isc system, which is present in mitochondria and utilizes ferredoxin as a reductant for Fe–S cluster biogenesis.<sup>84</sup>

The isolation of TrxA bound to Fe–S species was an unexpected finding in this study. The loss of TrxA oxidoreductase activity following *in vitro* cluster reconstitution, combined with the lack of cluster accumulation or activity of the TrxA Cys to Ala variants, suggests that Fe–S species are transiently ligated to the protein via the active site Cys residues. The nuclearity of this cluster along with the physiological relevance of this finding will be investigated in future studies. The accumulation of Fe–S species might be an artifact of high levels of expression in heterologous systems or possibly a mechanism for switching off active TrxA when present at high levels. Enzymes carrying dithiol reductase functions, such as glutaredoxins, can also coordinate transient Fe–S clusters, directing their functions in Fe–S metabolism as cluster carrier proteins.<sup>85–88</sup> It is possible that cluster coordination is not limited to glutaredoxins but also includes the thioredoxin family. A recent report demonstrated that both mitochondrial Trx isoforms from *Arabidopsis thaliana* were capable of coordinating a 4Fe–4S cluster, and this event required dimerization of the protein. Both Trx isoforms had standard disulfide reductase activity in the monomeric apo state; however, the activity of the reconstituted cluster-bound dimers was not evaluated.<sup>89</sup> The binding of a 2Fe–2S cluster has also been reported for a thioredoxin from the parasitic worm *Echinococcus granulosus*.<sup>90</sup> The coordination of Fe–S species to this form of thioredoxin led to the increased resistance of Trx from irreversible damage. The *E. granulosus* TrxA was able to complement a *Saccharomyces cerevisiae* Grx5-deficient strain, suggesting functional overlap between both

proteins. However, the *E. granulosus* Trx showed no activity–cluster binding relationship, as both the apo form and the holo form of the enzyme showed marginal activity in standard dithiol reductase assays. This result is in contrast to that for the *B. subtilis* TrxA, which showed a distinctly inverse activity–cluster binding profile, in which the apo form showed standard dithiol and persulfide reductase activities and the holo form was completely inactive. It is possible that TrxA is also involved in later stages of the biosynthetic process, including cluster assembly and delivery. The results from this study, however, provide experimental evidence of the occurrence of coupled reaction schemes involving the *B. subtilis* cysteine desulfurases and the thioredoxin system linking the formation and reduction of protein persulfides in the biogenesis of Fe–S clusters in this bacterium.

The reactivity of the *B. subtilis* Trx system in reducing persulfides accumulated within SufU and the impact of the Trx system on the activity of Fe–S enzymes suggest its involvement in Fe–S biogenesis. Preliminary analysis points to the reversible ligation of clusters on TrxA impacting the overall activity of the Trx system; however, the relevance of these initial findings needs to be further investigated in future studies. Nevertheless, *in vitro* kinetic analyses described in this study demonstrated that the rates of the reductase and desulfurase reactions are coupled, suggesting that the biogenesis of Fe–S clusters is dependent on the availability of cellular reducing equivalents.

## ■ ASSOCIATED CONTENT

### 📄 Supporting Information

The Supporting Information is available free of charge on the ACS Publications website at DOI: 10.1021/acs.biochem.9b00045.

A comprehensive list and description of primers, plasmids, and strains used in this study (Table S1), the intracellular concentrations of *B. subtilis* components involved in persulfide formation and reduction (Table S2), an estimation of *in vivo* reaction rates involving the formation and reduction of protein persulfides (Table S3), an alignment of thioredoxin and thioredoxin-like proteins found in selected bacterial genomes (Figure S1), absorption spectra of TrxR upon reduction by NADPH and NADH (Figure S2), the activity profile of the TrxR reaction (Figure S3), the activity profiles of the Trx system toward disulfide substrates (Figure S4), the growth impairment of *B. subtilis* PS832 and BEC28500 strains upon inactivation of Trx components (Figure S5), and the inhibitory effect of ebselen on the activity of thioredoxin reductase *in vitro* (Figure S6) (PDF)

### Accession Codes

TrxA, UniProtKB entry P14949; TrxR, UniProtKB entry P80880; SufS, UniProtKB entry O32164; SufU, UniProtKB entry O32163; YrvO, UniProtKB entry O34599; MnmA, UniProtKB entry O35020; YrkF, UniProtKB entry P54433.

## ■ AUTHOR INFORMATION

### Corresponding Authors

\*E-mail: kab2824@med.cornell.edu. Telephone: +1-336-404-3814.

\*E-mail: dossanpc@wfu.edu. Telephone: +1-336-758-3144.

### ORCID

Patricia C. Dos Santos: 0000-0002-3364-0931

### Author Contributions

C.Z., K.A.B., and W.G.T. contributed to the isolation and characterization of proteins described in this study. K.A.B., C.Z., and S.G. performed kinetic assays for disulfide substrates. C.Z., S.G., and P.K.P. performed kinetic assays for persulfide substrates. P.C.D.S. and K.A.B. conceived the idea. P.C.D.S. supervised students and managed the project. C.Z., K.A.B., and P.C.D.S. wrote the manuscript. All authors reviewed and edited the manuscript.

### Funding

C.Z. was a recipient of a graduate fellowship from the Wake Forest Center for Molecular Signaling. This research was sponsored by the National Science Foundation (1716535).

### Notes

The authors declare no competing financial interest.

### ABBREVIATIONS

Trx, thioredoxin; PLP, pyridoxal 5'-phosphate; DTT, dithiothreitol; TCEP, tris(2-carboxyethyl)phosphine; GSH, glutathione; GSSG, glutathione disulfide; Grx, glutaredoxin; NAD(P)H, nicotinamide adenine dinucleotide (phosphate); FAD, flavin adenine dinucleotide; EDTA, ethylenediaminetetraacetic acid; DTNB, 5,5'-dithiobis(2-nitrobenzoic acid); TNB, 2-nitro-5-thiobenzoate; IPTG, isopropyl  $\beta$ -D-1-thiogalactopyranoside; UV-vis, ultraviolet-visible; CRISPR, clustered regularly interspaced short palindromic repeats.

### REFERENCES

- (1) Hidese, R., Mihara, H., and Esaki, N. (2011) Bacterial cysteine desulfurases: versatile key players in biosynthetic pathways of sulfur-containing biofactors. *Appl. Microbiol. Biotechnol.* *91*, 47–61.
- (2) Mueller, E. G. (2006) Trafficking in persulfides: delivering sulfur in biosynthetic pathways. *Nat. Chem. Biol.* *2*, 185–194.
- (3) Zheng, L., White, R. H., Cash, V. L., and Dean, D. R. (1994) Mechanism for the desulfurization of L-cysteine catalyzed by the nifS gene product. *Biochemistry* *33*, 4714–4720.
- (4) Black, K. A., and Dos Santos, P. C. (2015) Shared-intermediates in the biosynthesis of thio-cofactors: Mechanism and functions of cysteine desulfurases and sulfur acceptors. *Biochim. Biophys. Acta, Mol. Cell Res.* *1853*, 1470–1480.
- (5) Behshad, E., and Bollinger, J. M., Jr. (2009) Kinetic analysis of cysteine desulfurase CD0387 from *Synechocystis* sp. PCC 6803: formation of the persulfide intermediate. *Biochemistry* *48*, 12014–12023.
- (6) Tirupati, B., Vey, J. L., Drennan, C. L., and Bollinger, J. M., Jr. (2004) Kinetic and structural characterization of Slr0077/SufS, the essential cysteine desulfurase from *Synechocystis* sp. PCC 6803. *Biochemistry* *43*, 12210–12219.
- (7) Kaiser, J. T., Clausen, T., Bourenkow, G. P., Bartunik, H. D., Steinbacher, S., and Huber, R. (2000) Crystal structure of a NifS-like protein from *Thermotoga maritima*: implications for iron sulphur cluster assembly. *J. Mol. Biol.* *297*, 451–464.
- (8) Cartini, F., Remelli, W., Dos Santos, P. C., Papenbrock, J., Pagani, S., and Forlani, F. (2011) Mobilization of sulfane sulfur from cysteine desulfurases to the *Azotobacter vinelandii* sulfurtransferase RhdA. *Amino Acids* *41*, 141–150.
- (9) Dai, Y., and Outten, F. W. (2012) The *E. coli* SufS-SufE sulfur transfer system is more resistant to oxidative stress than IscS-IscU. *FEBS Lett.* *586*, 4016–4022.
- (10) Kambampati, R., and Lauhon, C. T. (1999) IscS is a sulfurtransferase for the in vitro biosynthesis of 4-thiouridine in *Escherichia coli* tRNA. *Biochemistry* *38*, 16561–16568.
- (11) Selbach, B., Earles, E., and Dos Santos, P. C. (2010) Kinetic analysis of the bisubstrate cysteine desulfurase SufS from *Bacillus subtilis*. *Biochemistry* *49*, 8794–8802.

- (12) Rajakovich, L. J., Tomlinson, J., and Dos Santos, P. C. (2012) Functional Analysis of *Bacillus subtilis* Genes Involved in the Biosynthesis of 4-Thiouridine in tRNA. *J. Bacteriol.* *194*, 4933–4940.
- (13) Black, K. A., and Dos Santos, P. C. (2015) Abbreviated Pathway for Biosynthesis of 2-Thiouridine in *Bacillus subtilis*. *J. Bacteriol.* *197*, 1952–1962.
- (14) Bridwell-Rabb, J., Fox, N. G., Tsai, C. L., Winn, A. M., and Barondeau, D. P. (2014) Human frataxin activates Fe-S cluster biosynthesis by facilitating sulfur transfer chemistry. *Biochemistry* *53*, 4904–4913.
- (15) Mihara, H., Maeda, M., Fujii, T., Kurihara, T., Hata, Y., and Esaki, N. (1999) A nifS-like gene, csdB, encodes an *Escherichia coli* counterpart of mammalian selenocysteine lyase. Gene cloning, purification, characterization and preliminary X-ray crystallographic studies. *J. Biol. Chem.* *274*, 14768–14772.
- (16) Urbina, H. D., Silberg, J. J., Hoff, K. G., and Vickery, L. E. (2001) Transfer of Sulfur from IscS to IscU during Fe/S Cluster Assembly. *J. Biol. Chem.* *276*, 44521–44526.
- (17) Dunkle, J. A., Bruno, M., Outten, F. W., and Frantom, P. A. (2019) Structural evidence for dimer-interface driven regulation of the type II cysteine desulfurase, SufS. *Biochemistry* *58*, 687–696.
- (18) Selbach, B. P., Pradhan, P. K., and Dos Santos, P. C. (2013) Protected sulfur transfer reactions by the *Escherichia coli* Suf system. *Biochemistry* *52*, 4089–4096.
- (19) Fox, N. G., Chakrabarti, M., McCormick, S. P., Lindahl, P. A., and Barondeau, D. P. (2015) The Human Iron-Sulfur Assembly Complex Catalyzes the Synthesis of [2Fe-2S] Clusters on ISCU2 That Can Be Transferred to Acceptor Molecules. *Biochemistry* *54*, 3871–3879.
- (20) Dos Santos, P. C. (2014) Fe-S assembly in Gram-positive bacteria. In *Iron Sulfur Clusters in Chemistry and Biology* (Rouault, T., Ed.) pp 347–366, Verlag Walter de Gruyter, Berlin.
- (21) Dos Santos, P. C. (2017) *B. subtilis* as a Model for Studying the Assembly of Fe-S Clusters in Gram-Positive Bacteria. *Methods Enzymol.* *595*, 185–212.
- (22) Yokoyama, N., Nonaka, C., Ohashi, Y., Shioda, M., Terahata, T., Chen, W., Sakamoto, K., Maruyama, C., Saito, T., Yuda, E., Tanaka, N., Fujishiro, T., Kuzuyama, T., Asai, K., and Takahashi, Y. (2018) Distinct roles for U-type proteins in iron-sulfur cluster biosynthesis revealed by genetic analysis of the *Bacillus subtilis* sufCDSUB operon. *Mol. Microbiol.* *107*, 688–703.
- (23) Zheng, C., and Dos Santos, P. C. (2018) Metallocluster transactions: dynamic protein interactions guide the biosynthesis of Fe-S clusters in bacteria. *Biochem. Soc. Trans.* *46*, 1593–1603.
- (24) Outten, F. W., Wood, M. J., Munoz, F. M., and Storz, G. (2003) The SufE protein and the SufBCD complex enhance SufS cysteine desulfurase activity as part of a sulfur transfer pathway for Fe-S cluster assembly in *Escherichia coli*. *J. Biol. Chem.* *278*, 45713–45719.
- (25) Kim, J. H., Frederick, R. O., Reinen, N. M., Troupis, A. T., and Markley, J. L. (2013) [2Fe-2S]-ferredoxin binds directly to cysteine desulfurase and supplies an electron for iron-sulfur cluster assembly but is displaced by the scaffold protein or bacterial frataxin. *J. Am. Chem. Soc.* *135*, 8117–8120.
- (26) Sipos, K., Lange, H., Fekete, Z., Ullmann, P., Lill, R., and Kispal, G. (2002) Maturation of cytosolic iron-sulfur proteins requires glutathione. *J. Biol. Chem.* *277*, 26944–26949.
- (27) Lange, H., Kaut, A., Kispal, G., and Lill, R. (2000) A mitochondrial ferredoxin is essential for biogenesis of cellular iron-sulfur proteins. *Proc. Natl. Acad. Sci. U. S. A.* *97*, 1050–1055.
- (28) Rodriguez-Manzanique, M. T., Tamarit, J., Belli, G., Ros, J., and Herrero, E. (2002) Grx5 is a mitochondrial glutaredoxin required for the activity of iron/sulfur enzymes. *Mol. Biol. Cell* *13*, 1109–1121.
- (29) Johnson, D. C., Unciuleac, M. C., and Dean, D. R. (2006) Controlled expression and functional analysis of iron-sulfur cluster biosynthetic components within *Azotobacter vinelandii*. *J. Bacteriol.* *188*, 7551–7561.
- (30) Cai, K., Frederick, R. O., Tonelli, M., and Markley, J. L. (2018) Interactions of iron-bound frataxin with ISCU and ferredoxin on the

cysteine desulfurase complex leading to Fe-S cluster assembly. *J. Inorg. Biochem.* 183, 107–116.

(31) Webert, H., Freibert, S. A., Gallo, A., Heidenreich, T., Linne, U., Amlacher, S., Hurt, E., Muhlenhoff, U., Banci, L., and Lill, R. (2014) Functional reconstitution of mitochondrial Fe/S cluster synthesis on Isu1 reveals the involvement of ferredoxin. *Nat. Commun.* 5, 5013.

(32) Gaballa, A., Newton, G. L., Antelmann, H., Parsonage, D., Upton, H., Rawat, M., Claiborne, A., Fahey, R. C., and Helmann, J. D. (2010) Biosynthesis and functions of bacillithiol, a major low-molecular-weight thiol in Bacilli. *Proc. Natl. Acad. Sci. U. S. A.* 107, 6482–6486.

(33) Fang, Z., and Dos Santos, P. C. (2015) Protective role of bacillithiol in superoxide stress and Fe-S metabolism in *Bacillus subtilis*. *MicrobiologyOpen* 4, 616–631.

(34) Roberts, A. A., Sharma, S. V., Strankman, A. W., Duran, S. R., Rawat, M., and Hamilton, C. J. (2013) Mechanistic studies of FosB: a divalent metal-dependent bacillithiol-S-transferase that mediates fosfomycin resistance in *Staphylococcus aureus*. *Biochem. J.* 451, 69–79.

(35) Chandrangu, P., Dusi, R., Hamilton, C. J., and Helmann, J. D. (2014) Methylglyoxal resistance in *Bacillus subtilis*: contributions of bacillithiol-dependent and independent pathways. *Mol. Microbiol.* 91, 706–715.

(36) Posada, A. C., Kolar, S. L., Dusi, R. G., Francois, P., Roberts, A. A., Hamilton, C. J., Liu, G. Y., and Cheung, A. (2014) Importance of bacillithiol in the oxidative stress response of *Staphylococcus aureus*. *Infect. Immun.* 82, 316–332.

(37) Meyer, Y., Buchanan, B. B., Vignols, F., and Reichheld, J. P. (2009) Thioredoxins and glutaredoxins: unifying elements in redox biology. *Annu. Rev. Genet.* 43, 335–367.

(38) Holmgren, A., Johansson, C., Berndt, C., Lonn, M. E., Hudemann, C., and Lillig, C. H. (2005) Thiol redox control via thioredoxin and glutaredoxin systems. *Biochem. Soc. Trans.* 33, 1375–1377.

(39) Chan, C. M., Danchin, A., Marliere, P., and Sekowska, A. (2014) Paralogous metabolism: S-alkyl-cysteine degradation in *Bacillus subtilis*. *Environ. Microbiol.* 16, 101–117.

(40) Burguier, P., Auger, S., Hullo, M. F., Danchin, A., and Martin-Verstraete, I. (2004) Three different systems participate in L-cystine uptake in *Bacillus subtilis*. *J. Bacteriol.* 186, 4875–4884.

(41) Kobayashi, K., Ehrlich, S. D., Albertini, A., Amati, G., Andersen, K. K., Arnaud, M., Asai, K., Ashikaga, S., Aymerich, S., Bessieres, P., Boland, F., Brignell, S. C., Bron, S., Bunai, K., Chapuis, J., Christiansen, L. C., Danchin, A., Debarbouille, M., Dervyn, E., Deurling, E., Devine, K., Devine, S. K., Dreesen, O., Errington, J., Fillingner, S., Foster, S. J., Fujita, Y., Galizzi, A., Gardan, R., Eschevin, C., Fukushima, T., Haga, K., Harwood, C. R., Hecker, M., Hosoya, D., Hullo, M. F., Kakeshita, H., Karamata, D., Kasahara, Y., Kawamura, F., Koga, K., Koski, P., Kuwana, R., Imamura, D., Ishimaru, M., Ishikawa, S., Ishio, I., Le Coq, D., Masson, A., Mauel, C., Meima, R., Mellado, R. P., Moir, A., Moriya, S., Nagakawa, E., Nanamiya, H., Nakai, S., Nygaard, P., Ogura, M., Ohanan, T., O'Reilly, M., O'Rourke, M., Pragai, Z., Pooley, H. M., Rapoport, G., Rawlins, J. P., Rivas, L. A., Rivolta, C., Sadaie, A., Sadaie, Y., Sarvas, M., Sato, T., Saxild, H. H., Scanlan, E., Schumann, W., Seegers, J. F., Sekiguchi, J., Sekowska, A., Seror, S. J., Simon, M., Stragier, P., Studer, R., Takamatsu, H., Tanaka, T., Takeuchi, M., Thomaidis, H. B., Vagner, V., van Dijk, J. M., Watabe, K., Wipat, A., Yamamoto, H., Yamamoto, M., Yamamoto, Y., Yamane, K., Yata, K., Yoshida, K., Yoshikawa, H., Zuber, U., and Ogasawara, N. (2003) Essential *Bacillus subtilis* genes. *Proc. Natl. Acad. Sci. U. S. A.* 100, 4678–4683.

(42) Scharf, C., Riethdorf, S., Ernst, H., Engelmann, S., Volker, U., and Hecker, M. (1998) Thioredoxin is an essential protein induced by multiple stresses in *Bacillus subtilis*. *J. Bacteriol.* 180, 1869–1877.

(43) Holmgren, A. (1979) Thioredoxin catalyzes the reduction of insulin disulfides by dithiothreitol and dihydrolipoamide. *J. Biol. Chem.* 254, 9627–9632.

(44) Poole, L. B. (2015) The basics of thiols and cysteines in redox biology and chemistry. *Free Radical Biol. Med.* 80C, 148–157.

(45) Collet, J. F., and Messens, J. (2010) Structure, function, and mechanism of thioredoxin proteins. *Antioxid. Redox Signaling* 13, 1205–1216.

(46) Crow, A., Liu, Y., Möller, M. C., Le Brun, N. E., and Hederstedt, L. (2009) Structure and functional properties of *Bacillus subtilis* endospore biogenesis factor StoA. *J. Biol. Chem.* 284, 10056–10066.

(47) Bukowska-Faniband, E., and Hederstedt, L. (2017) Transpeptidase activity of penicillin-binding protein SpoVD in peptidoglycan synthesis conditionally depends on the disulfide reductase StoA. *Mol. Microbiol.* 105, 98–114.

(48) Arnaouteli, S., Ferreira, A. S., Schor, M., Morris, R. J., Bromley, K. M., Jo, J., Cortez, K. L., Sukhodub, T., Prescott, A. R., Dietrich, L. E. P., MacPhee, C. E., and Stanley-Wall, N. R. (2017) Bifunctionality of a biofilm matrix protein controlled by redox state. *Proc. Natl. Acad. Sci. U. S. A.* 114, E6184–E6191.

(49) Parker, M. J., Zhu, X., and Stubbe, J. (2014) *Bacillus subtilis* class Ib ribonucleotide reductase: high activity and dynamic subunit interactions. *Biochemistry* 53, 766–776.

(50) Mostertz, J., Hochgrafe, F., Jurgen, B., Schweder, T., and Hecker, M. (2008) The role of thioredoxin TrxA in *Bacillus subtilis*: a proteomics and transcriptomics approach. *Proteomics* 8, 2676–2690.

(51) Möller, M. C., and Hederstedt, L. (2008) Extracytoplasmic processes impaired by inactivation of *trxA* (thioredoxin gene) in *Bacillus subtilis*. *J. Bacteriol.* 190, 4660–4665.

(52) Smits, W. K., Dubois, J. Y., Bron, S., van Dijk, J. M., and Kuipers, O. P. (2005) Tricky business: transcriptome analysis reveals the involvement of thioredoxin A in redox homeostasis, oxidative stress, sulfur metabolism, and cellular differentiation in *Bacillus subtilis*. *J. Bacteriol.* 187, 3921–3930.

(53) Peters, J. M., Colavin, A., Shi, H., Czarny, T. L., Larson, M. H., Wong, S., Hawkins, J. S., Lu, C. H. S., Koo, B. M., Marta, E., Shiver, A. L., Whitehead, E. H., Weissman, J. S., Brown, E. D., Qi, L. S., Huang, K. C., and Gross, C. A. (2016) A Comprehensive, CRISPR-based Functional Analysis of Essential Genes in Bacteria. *Cell* 165, 1493–1506.

(54) Bradford, M. M. (1976) A rapid and sensitive method for the quantitation of microgram quantities of protein utilizing the principle of protein-dye binding. *Anal. Biochem.* 72, 248–254.

(55) Outten, F. W., Djaman, O., and Storz, G. (2004) A *suf* operon requirement for Fe-S cluster assembly during iron starvation in *Escherichia coli*. *Mol. Microbiol.* 52, 861–872.

(56) Fultz, P. N., and Kemper, J. (1981) Wild-type isopropylmalate isomerase in *Salmonella typhimurium* is composed of two different subunits. *J. Bacteriol.* 148, 210–219.

(57) Manikandan, K., Geerlof, A., Zozulya, A. V., Svergun, D. I., and Weiss, M. S. (2011) Structural studies on the enzyme complex isopropylmalate isomerase (LeuCD) from *Mycobacterium tuberculosis*. *Proteins: Struct., Funct., Genet.* 79, 35–49.

(58) Alen, C., and Sonenshein, A. L. (1999) *Bacillus subtilis* acnitolase is an RNA-binding protein. *Proc. Natl. Acad. Sci. U. S. A.* 96, 10412–10417.

(59) Gu, M., and Imlay, J. A. (2013) Superoxide poisons mononuclear iron enzymes by causing mismetallation. *Mol. Microbiol.* 89, 123–134.

(60) Bowater, L., Fairhurst, S. A., Just, V. J., and Bornemann, S. (2004) *Bacillus subtilis* YxaG is a novel Fe-containing quercetin 2,3-dioxygenase. *FEBS Lett.* 557, 45–48.

(61) Martin, H. L., Black, K. A., and Dos Santos, P. C. (2016) Functional investigation of *Bacillus subtilis* YrkF's involvement in sulfur transfer reactions. *Peptidomics* 34, 54.

(62) Selbach, B. P., Chung, A. H., Scott, A. D., George, S. J., Cramer, S. P., and Dos Santos, P. C. (2014) Fe-S cluster biogenesis in Gram-positive bacteria: SufU is a zinc-dependent sulfur transfer protein. *Biochemistry* 53, 152–160.

(63) Siegel, L. M. (1965) A Direct Microdetermination for Sulfide. *Anal. Biochem.* 11, 126–132.

(64) Williams, C. H., Jr. (1995) Mechanism and structure of thioredoxin reductase from *Escherichia coli*. *FASEB J.* 9, 1267–1276.

- (65) Gustafsson, T. N., Sahlin, M., Lu, J., Sjöberg, B. M., and Holmgren, A. (2012) *Bacillus anthracis* thioredoxin systems, characterization and role as electron donors for ribonucleotide reductase. *J. Biol. Chem.* 287, 39686–39697.
- (66) Baker, L. M., Raudonikiene, A., Hoffman, P. S., and Poole, L. B. (2001) Essential thioredoxin-dependent peroxiredoxin system from *Helicobacter pylori*: genetic and kinetic characterization. *J. Bacteriol.* 183, 1961–1973.
- (67) Mulrooney, S. B., and Williams, C. H., Jr. (1997) Evidence for two conformational states of thioredoxin reductase from *Escherichia coli*: use of intrinsic and extrinsic quenchers of flavin fluorescence as probes to observe domain rotation. *Protein Sci.* 6, 2188–2195.
- (68) Gustafsson, T. N., Sandalova, T., Lu, J., Holmgren, A., and Schneider, G. (2007) High-resolution structures of oxidized and reduced thioredoxin reductase from *Helicobacter pylori*. *Acta Crystallogr., Sect. D: Biol. Crystallogr.* 63, 833–843.
- (69) Lennon, B. W., and Williams, C. H., Jr. (1997) Reductive half-reaction of thioredoxin reductase from *Escherichia coli*. *Biochemistry* 36, 9464–9477.
- (70) Holmgren, A. (1979) Reduction of disulfides by thioredoxin. Exceptional reactivity of insulin and suggested functions of thioredoxin in mechanism of hormone action. *J. Biol. Chem.* 254, 9113–9119.
- (71) Peng, H., Zhang, Y., Trinidad, J. C., and Giedroc, D. P. (2018) Thioredoxin Profiling of Multiple Thioredoxin-Like Proteins in *Staphylococcus aureus*. *Front. Microbiol.* 9, 2385.
- (72) Peng, H., Zhang, Y., Palmer, L. D., Kehl-Fie, T. E., Skaar, E. P., Trinidad, J. C., and Giedroc, D. P. (2017) Hydrogen Sulfide and Reactive Sulfur Species Impact Proteome S-Sulfhydration and Global Virulence Regulation in *Staphylococcus aureus*. *ACS Infect. Dis.* 3, 744–755.
- (73) Kouwen, T. R., Andrell, J., Schrijver, R., Dubois, J. Y., Maher, M. J., Iwata, S., Carpenter, E. P., and van Dijl, J. M. (2008) Thioredoxin A active-site mutants form mixed disulfide dimers that resemble enzyme-substrate reaction intermediates. *J. Mol. Biol.* 379, 520–534.
- (74) Moore, E. C., Reichard, P., and Thelander, L. (1964) Enzymatic Synthesis of Deoxyribonucleotides.V. Purification and Properties of Thioredoxin Reductase from *Escherichia coli* B. *J. Biol. Chem.* 239, 3445–3452.
- (75) Doka, E., Pader, I., Biro, A., Johansson, K., Cheng, Q., Ballago, K., Prigge, J. R., Pastor-Flores, D., Dick, T. P., Schmidt, E. E., Arner, E. S., and Nagy, P. (2016) A novel persulfide detection method reveals protein persulfide- and polysulfide-reducing functions of thioredoxin and glutathione systems. *Sci. Adv.* 2, e1500968.
- (76) Wedmann, R., Onderka, C., Wei, S., Szijarto, I. A., Miljkovic, J. L., Mitrovic, A., Lange, M., Savitsky, S., Yadav, P. K., Torregrossa, R., Harrer, E. G., Harrer, T., Ishii, I., Gollasch, M., Wood, M. E., Galardon, E., Xian, M., Whiteman, M., Banerjee, R., and Filipovic, M. R. (2016) Improved tag-switch method reveals that thioredoxin acts as depersulfidase and controls the intracellular levels of protein persulfidation. *Chem. Sci.* 7, 3414–3426.
- (77) Libiad, M., Motl, N., Akey, D. L., Sakamoto, N., Fearon, E. R., Smith, J. L., and Banerjee, R. (2018) Thiosulfate sulfurtransferase-like domain-containing I protein interacts with thioredoxin. *J. Biol. Chem.* 293, 2675–2686.
- (78) Albrecht, A. G., Netz, D. J., Miethke, M., Pierik, A. J., Burghaus, O., Peuckert, F., Lill, R., and Marahiel, M. A. (2010) SufU is an essential iron-sulfur cluster scaffold protein in *Bacillus subtilis*. *J. Bacteriol.* 192, 1643–1651.
- (79) Gustafsson, T. N., Osman, H., Werngren, J., Hoffner, S., Engman, L., and Holmgren, A. (2016) Ebselen and analogs as inhibitors of *Bacillus anthracis* thioredoxin reductase and bactericidal antibacterials targeting *Bacillus* species. *Biochim. Biophys. Acta, Gen. Subj.* 1860, 1265–1271.
- (80) Luo, Z., Sheng, J., Sun, Y., Lu, C., Yan, J., Liu, A., Luo, H. B., Huang, L., and Li, X. (2013) Synthesis and evaluation of multi-target-directed ligands against Alzheimer's disease based on the fusion of donepezil and ebselen. *J. Med. Chem.* 56, 9089–9099.
- (81) Fujishiro, T., Terahata, T., Kunichika, K., Yokoyama, N., Maruyama, C., Asai, K., and Takahashi, Y. (2017) Zinc-Ligand Swapping Mediated Complex Formation and Sulfur Transfer between SufS and SufU for Iron-Sulfur Cluster Biogenesis in *Bacillus subtilis*. *J. Am. Chem. Soc.* 139, 18464–18467.
- (82) Zhu, B., and Stulke, J. (2018) SubtiWiki in 2018: from genes and proteins to functional network annotation of the model organism *Bacillus subtilis*. *Nucleic Acids Res.* 46, D743–D748.
- (83) Yu, A. C., Loo, J. F., Yu, S., Kong, S. K., and Chan, T. F. (2014) Monitoring bacterial growth using tunable resistive pulse sensing with a pore-based technique. *Appl. Microbiol. Biotechnol.* 98, 855–862.
- (84) Braymer, J. J., Stumpfig, M., Thelen, S., Muhlenhoff, U., and Lill, R. (2019) Depletion of thiol reducing capacity impairs cytosolic but not mitochondrial iron-sulfur protein assembly machineries. *Biochim. Biophys. Acta, Mol. Cell Res.* 1866, 240–251.
- (85) Rouhier, N., Unno, H., Bandyopadhyay, S., Masip, L., Kim, S. K., Hirasawa, M., Gualberto, J. M., Lattard, V., Kusunoki, M., Knaff, D. B., Georgiou, G., Hase, T., Johnson, M. K., and Jacquot, J. P. (2007) Functional, structural, and spectroscopic characterization of a glutathione-ligated [2Fe-2S] cluster in poplar glutaredoxin C1. *Proc. Natl. Acad. Sci. U. S. A.* 104, 7379–7384.
- (86) Roret, T., Tsan, P., Couturier, J., Zhang, B., Johnson, M. K., Rouhier, N., and Didierjean, C. (2014) Structural and spectroscopic insights into BolA-glutaredoxin complexes. *J. Biol. Chem.* 289, 24588–24598.
- (87) Zhang, B., Bandyopadhyay, S., Shakamuri, P., Naik, S. G., Huynh, B. H., Couturier, J., Rouhier, N., and Johnson, M. K. (2013) Monothiol glutaredoxins can bind linear [Fe3S4]+ and [Fe4S4]2+ clusters in addition to [Fe2S2]2+ clusters: spectroscopic characterization and functional implications. *J. Am. Chem. Soc.* 135, 15153–15164.
- (88) Molina-Navarro, M. M., Casas, C., Piedrafita, L., Belli, G., and Herrero, E. (2006) Prokaryotic and eukaryotic monothiol glutaredoxins are able to perform the functions of Grx5 in the biogenesis of Fe/S clusters in yeast mitochondria. *FEBS Lett.* 580, 2273–2280.
- (89) Zannini, F., Roret, T., Przybyla-Toscano, J., Dhalleine, T., Rouhier, N., and Couturier, J. (2018) Mitochondrial Arabidopsis thaliana TRXo Isoforms Bind an Iron(-)Sulfur Cluster and Reduce NFU Proteins In Vitro. *Antioxidants* 7, 142.
- (90) Bisio, H., Bonilla, M., Manta, B., Grana, M., Salzman, V., Aguilar, P. S., Gladyshev, V. N., Comini, M. A., and Salinas, G. (2016) A New Class of Thioredoxin-Related Protein Able to Bind Iron-Sulfur Clusters. *Antioxid. Redox Signaling* 24, 205–216.